*

Suppression to Radial Force and Torque Ripple of Concentrated PMSM with Double Independent Three-Phase Windings

Takumi Soeda*, and Hitoshi Haga*
* Dept. of Electrical, Electronics and Information Engineering, Nagaoka Univ. of Technology, Nagaoka Niigata pref., Japan

Abstract—**This paper proposes a machine structure and control method for low vibration of PMSM. Torque ripple and radial force cause vibration. Sixth-order torque and sixth-order radial force are the focus of attention in this paper. However, it is difficult to suppress to them by using the conventional inverter driven PMSM structure. Therefore, this paper proposes that the degree of freedom has been increased by adopting multiple winding with winding deviations. The proposed method suppresses the sixth-order radial force by superimposition of harmonic current and negate the sixth-order torque by the PMSM structure. The proposed method was confirmed by simulation and experiment. The radial force is evaluated by measuring the radial acceleration on the motor surface. The sixth-order component of the acceleration in the radial direction was reduced by 73.3%. The sixth-order torque component is smaller than the main torque component, for this reason, it was suppressed by its structural characteristics.**

Index Terms— **Phase shifted double star IPMSM, vibration, torque ripple, radial force**

I. INTRODUCTION

Permanent Magnet Synchronous Machines (PMSM) are used in various applications such as industrial and automotive. The PMSM is useful because it is small, lightweight, and high controllability, however it causes vibration [1]. PMSM is sometimes used in systems where the distance between the equipment and the user is short, including the steering assist motor for electric power steering of vehicles. In such a case, the vibration caused by PMSM may give the user an unpleasant feeling due to the generation of noise. In particular, in the steering of a vehicle, since the driver directly grips the steering wheel, which not only causes discomfort, but also may hinder driving. Therefore, in such a system, it is desirable that the PMSM vibration and noise be as low as possible.

There are two main causes of vibration caused by PMSM. One is torque ripple that occurs mainly in the 6th-order electrical angle and its integral multiples [2]. Sixth-order electrical angle torque ripple tend to occur more than higher-order torque ripples. The other is an electromagnetic force in the radial direction (also known as radial force [3]) that occurs at even-numbered electrical angle [4]. Among them, the sixth-order component of the zero-order annular mode vibration of the circular ring which causes mechanical motion that expands and contracts the radius of the machine stator, and is likely to appear as sound noise [5]. As described above, the electrical angle 6th torque ripple and the electrical angle 6th radial force are required to be reduced in order to improve the steering feel. (Hereinafter, for convenience, when expressed as n-th order, it means that the electrical angle is n-th order.)

Generally, the radial force is larger when the PMSM stator is concentrated winding than distributed winding [4]. On the other hand, the concentrated winding stator has a simpler structure than the distributed winding stator, and therefore the concentrated winding is preferable because it can reduce the cost.

As a torque ripple suppression method, there are methods by structural optimization [6] such as improvement of magnet arrangement and skew addition, but the method of suppression by control is simple and desirable. It is known that in a general three-phase PMSM, suppression of sixth-order torque ripple can be achieved by superimposing the sixth-order harmonic current component on the q-axis current [2][7]. On the other hand, the 6th radial force can be achieved by superimposing the 6th harmonic current component on the d-axis or q-axis current [8]. However, since the phase of the 6th current for suppressing the 6th torque ripple and the phase of the 6th current for suppressing the 6th radial force do not always match, simultaneous suppression becomes a problem. Therefore, it is difficult to suppress both by superimposing current, and another approach is required.

High reliability is also an important issue for in-vehicle equipment [9]. Multiplexing of power converters and multiplexing of windings are used as an approach to improving reliability and fail-safe motor drive [10][11][12].

Therefore, in this paper, a control method for torque ripple and radial force suppression of a concentrated winding PMSM having two independent three-phase windings that share a common DC power supply was examined. The target system ensures redundancy and improves reliability, and uses the structural features and control freedom to superimpose the sixth harmonic current to suppress sixth-order torque ripple and sixth-order radial force. The effectiveness of the proposed control method is verified by simulations and experiments.

The sixth-order radial force component of a double-winding motor with winding displacement is in opposite phase between winding sets depending on the conditions, and theoretically cancels each other out. However, in

*

reality, the motor cases are not rigid and do not completely cancel each other out due to factors such as the fixing method, so it is still important to suppress the sixth-order radial force that causes the zeroth-order annular mode vibration.

II. PMSM Control Method

A. Motor Specification

Fig. 1 shows the motor winding structure used in this paper.

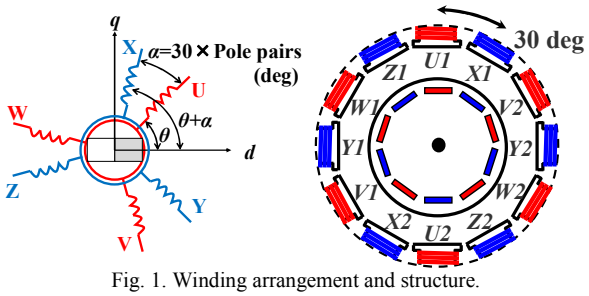

Fig. 1. Winding arrangement and structure.

The machine has two sets of three-phase windings, [u, v, w] and [x, y, z] phases, respectively. There is a winding misalignment between each winding set, and this motor has a mechanical angle deviation of 30 degrees. The number of pole pairs must be odd as a condition for suppressing the sixth-order torque ripple. The sum of the sixth-order torque ripple T_{6th} output by each winding sets (A, B) is

$$T_{6\mathrm{th}} = T_{A6th}\sin(6\theta) + T_{B6th}\sin\{6(\theta + P_n\alpha_m)\}. \quad (1)$$

where, T_{n6th} is amplitude of sixth-order torque ripple (n=A, B), α_m is the winding displacement in mechanical angle, and P_n is the number of pole pair. When the sixth-order torque ripple amplitudes output by each winding set are equal, they cancel each other out when the number of pole pairs is odd, and they strengthen each other when it is even. Therefore, in this paper, by adopting a machine with a structure of 5 pole pairs and 12 slots, the sixth-order torque ripples cancel each other out.

B. Control Scheme and Decoupling

Since a double-winding machine with winding deviation causes magnetic interference between windings, it is difficult to control it using two general d-q reference frames. Therefore, the decoupling method shown in [13] and [14] is adopted. Magnetic decoupling is performed by using the general rotation coordinate transformation matrix for the d-q reference frame

$$\boldsymbol{T}_{\mathrm{P}}(\delta) = \sqrt{\frac{2}{3}}\begin{bmatrix} \cos(\delta) & \cos\left(\delta - \frac{2\pi}{3}\right) & \cos\left(\delta + \frac{2\pi}{3}\right) \\ -\sin(\delta) & -\sin\left(\delta - \frac{2\pi}{3}\right) & -\sin\left(\delta + \frac{2\pi}{3}\right) \end{bmatrix} \quad (2)$$

and the transformation matrix for transforming the new rotation coordinates (D-Q reference frames) in

$$\boldsymbol{T}_{DQ}(\theta) = \frac{1}{\sqrt{2}}\begin{bmatrix} \boldsymbol{T}_P(\theta) & \boldsymbol{T}_P(\theta - \alpha) \\ \boldsymbol{T}_P\left(\theta + \frac{\pi}{2}\right) & \boldsymbol{T}_P\left(\theta - \alpha - \frac{\pi}{2}\right) \end{bmatrix}. \quad (3)$$

Where, θ is electrical angle and α is the winding displacement in electrical angle. This coordinate transformation is obtained by diagonalizing the inductance matrix in d-q reference frames. From the above, four D-Q axes $[D_1, Q_1, D_2, Q_2]$ are defined. The D1-Q1 reference frame obtained by this conversion corresponds to the d-axis and the q-axis of the general d-q reference frames, and corresponds to the magnetic flux direction and the orthogonal direction respectively. The D2-Q2 reference frame correspond to the redundant degrees of freedom, and the reference currents in D2-Q2 reference frame is controlled to be zero. Due to the coordinate transformation to the D-Q reference frames, the inductance matrix of the double three-phase PMSM becomes a diagonal matrix as shown in

$$\boldsymbol{L_{DQ}} = \begin{bmatrix} L_{D1} & 0 & 0 & 0 \\ 0 & L_{Q1} & 0 & 0 \\ 0 & 0 & L_{D2} & 0 \\ 0 & 0 & 0 & L_{Q2} \end{bmatrix} \quad (4)$$

where, the matrix elements are the synchronous inductance of PMSM. Under these assumption, the flux linkage equation is

$$\begin{bmatrix} \psi_{D1} \\ \psi_{Q1} \\ \psi_{D2} \\ \psi_{Q2} \end{bmatrix} = \boldsymbol{L_{DQ}}\begin{bmatrix} i_{D1} \\ i_{Q1} \\ i_{D2} \\ i_{Q2} \end{bmatrix} + \begin{bmatrix} \sqrt{3}\psi_{PM} \\ 0 \\ 0 \\ 0 \end{bmatrix} \quad (5)$$

where, ψ_{PM} is flux of permanent magnet. Since the inductance matrix is diagonal, there is no coupling exists between the reference frames.

III. Radial Force Suppression Control Method

A. Current Reference

As mentioned in the previous section, the D2-Q2 reference frame has redundant degrees of freedom. The suppression of the sixth-order radial force can be achieved by superimposing the 6th harmonic current on the D2-Q2 reference frame. Also, considering that the D1-Q1 reference frame correspond to the d-q reference frames of general PMSM, it is not preferable to superimpose the harmonic current on them. From the above, current command I_{DQ*} in the D-Q reference frames is

$$\boldsymbol{I_{DQ*}} = [I_{D1} \quad I_{Q1} \quad I_{6th}\cos(6\theta + \theta_{6th}) \quad I_{6th}\sin(6\theta + \theta_{6th})]^T, \quad (6)$$

where, I_{D1} and I_{Q1} are values determined based on the torque command value or speed command value, I_{6th} and θ_{6th} are the amplitude and phase of the superimposed harmonic current. In this paper, to verify the basic theory, the I_{D1} current command value was evaluated as 0 based on $I_d = 0$ control. In the machine with the winding structure adopted in this paper, even if a current such as that given by equation (6) is applied to the D2-Q2 reference frame, it cancels out between the winding sets, for this reason, there is no effect on the output torque.

B. Harmonic Current Control Method

PI control, which is often used in current control, cannot

*

follow the sine wave command or suppress the sine wave disturbance due to the internal model principle, and a steady-state error is generated. Therefore, in this paper, a PIR controller that adds a resonant controller (R controller) in addition to the PI controller is used in order to track the harmonic current command [15]. The PI controller and R controller are

$$G_{PI}(s) = K_p\left(1+\frac{1}{T_i s}\right), \tag{7}$$

$$G_R(s) = \frac{2K_r\omega_c s}{s^2+2\omega_c s+(6\omega_e)^2}. \tag{8}$$

Where, K_p is proportional gain, T_i is integration time, ω_c is cutoff frequency, and ω_e is electric frequency.

The R controller has a high gain with a frequency component 6 times the electrical angular frequency ω_e, and the response peak width is determined by the cutoff frequency. The characteristics of the R controller are easy to adjust because the characteristics of controller is determined by the product of the gain K_r and the cutoff frequency ω_c. Fig. 2 shows the control block.

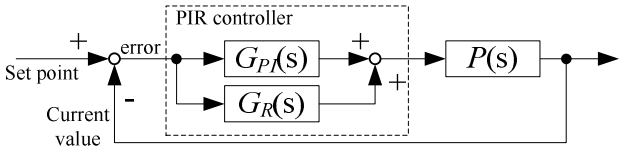

Fig. 2. PIR controller in feedback system.

The frequency characteristics of the closed-loop transfer function are shown in Fig. 3.

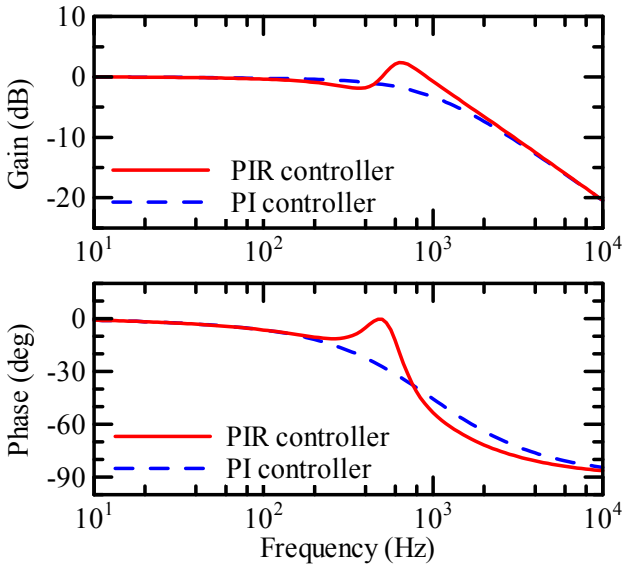

Fig. 3. Frequency response of feedback system for 1st-order lagging plant. Left graphs are PI controller, Right graphs are PIR controller.

In Fig. 3, since the electrical angular frequency is 100 Hz, the gain becomes high at 600 Hz, which is six times that of the R controller.

For the gain design of the R controller, the phase margin of the feedback system of the PIR controller and the first-order lag element simulating the machine was simulated, and sufficient margin was set.

IV. Simulation

Evaluate the radial force and torque of the machine using FEM analysis. Table 1 shows the simulation parameters.

TABLE I
Machine Parameters and Simulation Conditions

Symbol	Quantity	Parameter
N	Machine speed	1200 rpm
P_n	Pole pairs	5
S	Slot number	12
n	Winding turns	8
I_{D1}	I_{D1} reference	0 A
I_{Q1}	I_{Q1} reference	10 A
I_{6th}	6th current amplitude	8.8 A
θ_{6th}	6th current phase	285 deg
α	Winding displacement	150 deg
V_{dc}	DC voltage	12 V
f_s	Switching frequency	20 kHz
L_{D1}	D1 inductance	131 μH
L_{Q1}	Q1 inductance	198 μH
L_{D2}	D2 inductance	98.8 μH
L_{Q2}	Q2 inductance	90.1 μH

The machine assumes a constant torque output and externally applies a constant speed rotation to the rotor. In order to output a constant torque, I_{Q1} corresponding to the torque axis is controlled with a constant value. The radial force was evaluated by measuring the electromagnetic excitation force applied to the center of the U-phase tooth tip and analyzing its harmonics. The torque was evaluated by harmonic analysis. Since the sixth-order radial force to be canceled depends on the output torque of the machine, the sixth-order current amplitude and phase that minimize the radial force are searched for by simulation and determined.

A. Verification using an ideal current source

A simulation was performed using an ideal current source in order to evaluate the suppression of the sixth-order radial force by superimposing the sixth-order harmonic current. Fig. 4 shows the harmonic analysis results of the radial force with and without the presence of the sixth-order harmonic current in the D2-Q2 frames.

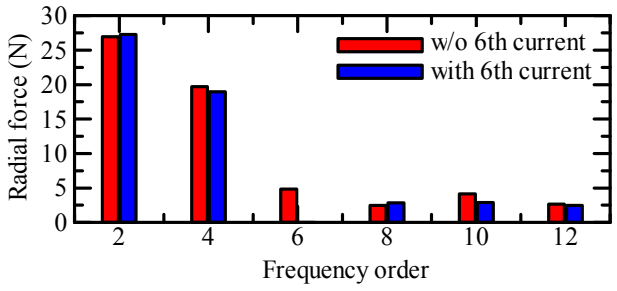

Fig. 4. Harmonic analysis of radial force with an ideal current source.

Since the machine synchronous frequency is 100 Hz, the sixth-order radial force appears at 600 Hz. The sixth-order radial force improved from 4.86 N to 0.0151 N, and reduction of 99.7 % was confirmed.

*

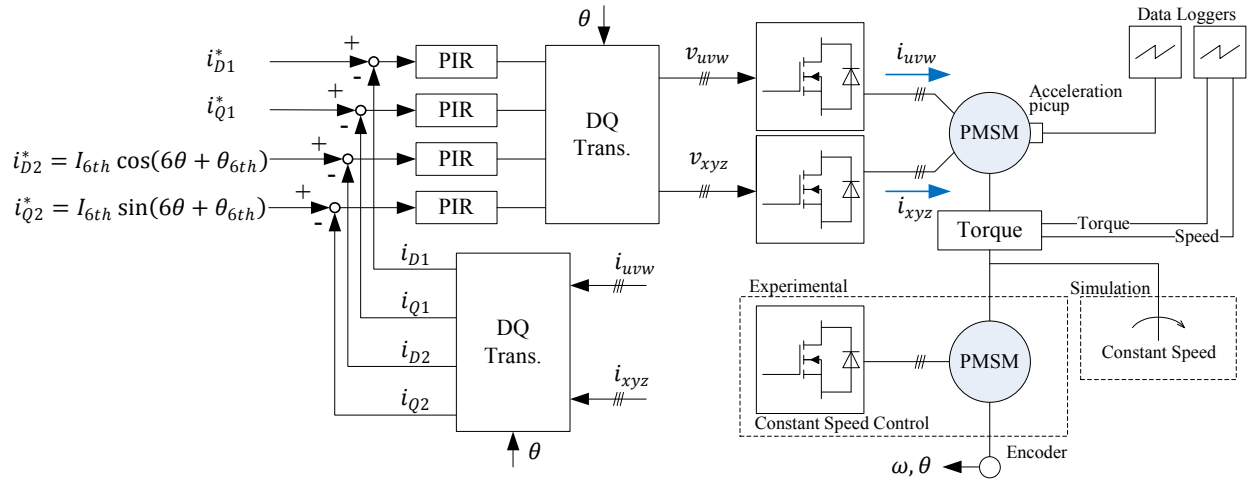

Fig. 5. Experimental setup and simulation model for evaluation radial force and torque ripple

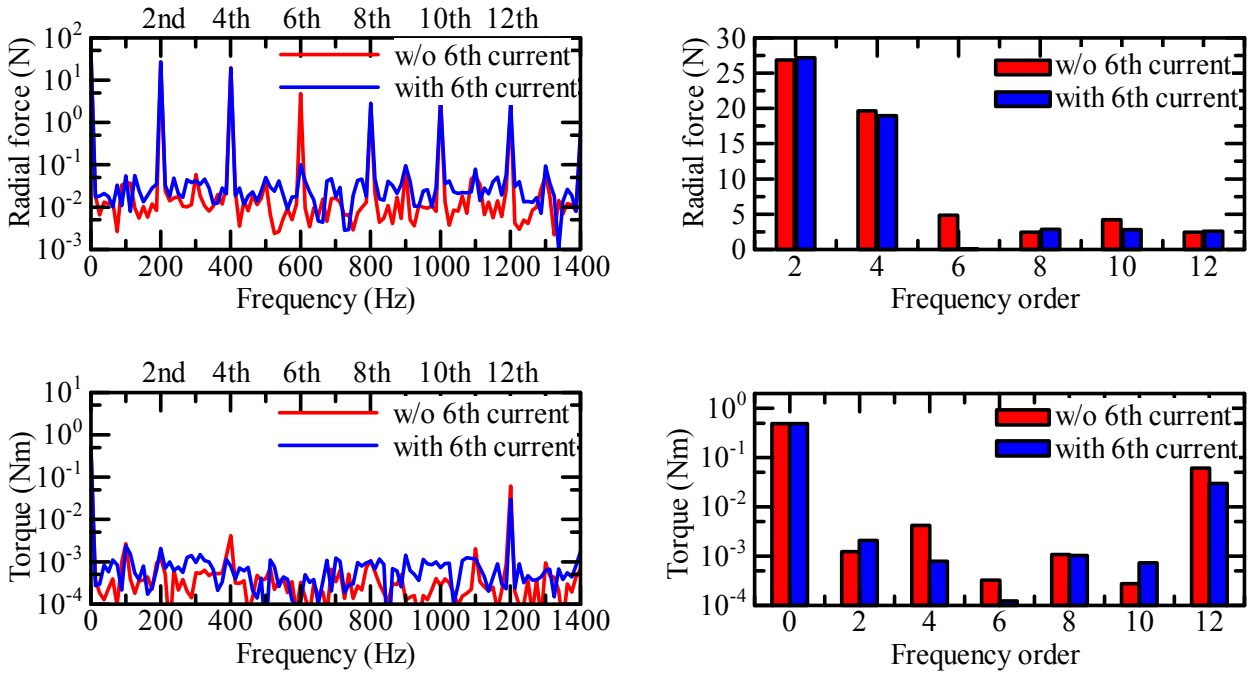

Fig. 6. Simulation results of radial force harmonic contents (upper graphs) and torque harmonic contents (lower graphs).

B. Evaluation by voltage source inverter

A system using a voltage inverter and current controller was evaluated to simulate actual operation. Fig. 5 presents the block diagram of the proposed system. A PIR controller is used as the current controller. Fig. 6 shows the results of harmonic analysis of radial force and torque with and without the sixth-order harmonic current.

The sixth-order radial force appearing at 600 Hz was improved from 4.82 N to 0.101 N, which was confirmed to be reduced by 97.9 %. On the other hand, the sixth-order torque ripple is 3.27×10^{-4} Nm (w/o 6th current) and 3.27×10^{-4} Nm (with 6th current), which is extremely small compared to the main torque component (zeroth-order torque) and the twelfth-order torque component. Therefore, it is considered that the structure suppresses the sixth-order torque ripple.

V. EXPERIMENT

Experimentally evaluate the radial force and torque of the machine. Radial force cannot be measured directly because it is a dimension of force. Therefore, the radial force is evaluated by measuring the radial acceleration on the surface of the machine case.

Fig. 5 presents the block diagram of the proposed system. The test machine is rotated at a constant speed using the PMSM installed opposite. Similar to the simulation, the I_{Q1} current corresponding to the torque axis is controlled at a constant value in order to output a constant torque. For the amplitude and phase of the superimposed sixth-order current, the values obtained by searching in advance by preliminary experiments are used.

Table 2 shows the conditions and parameters using in the experiment.

*

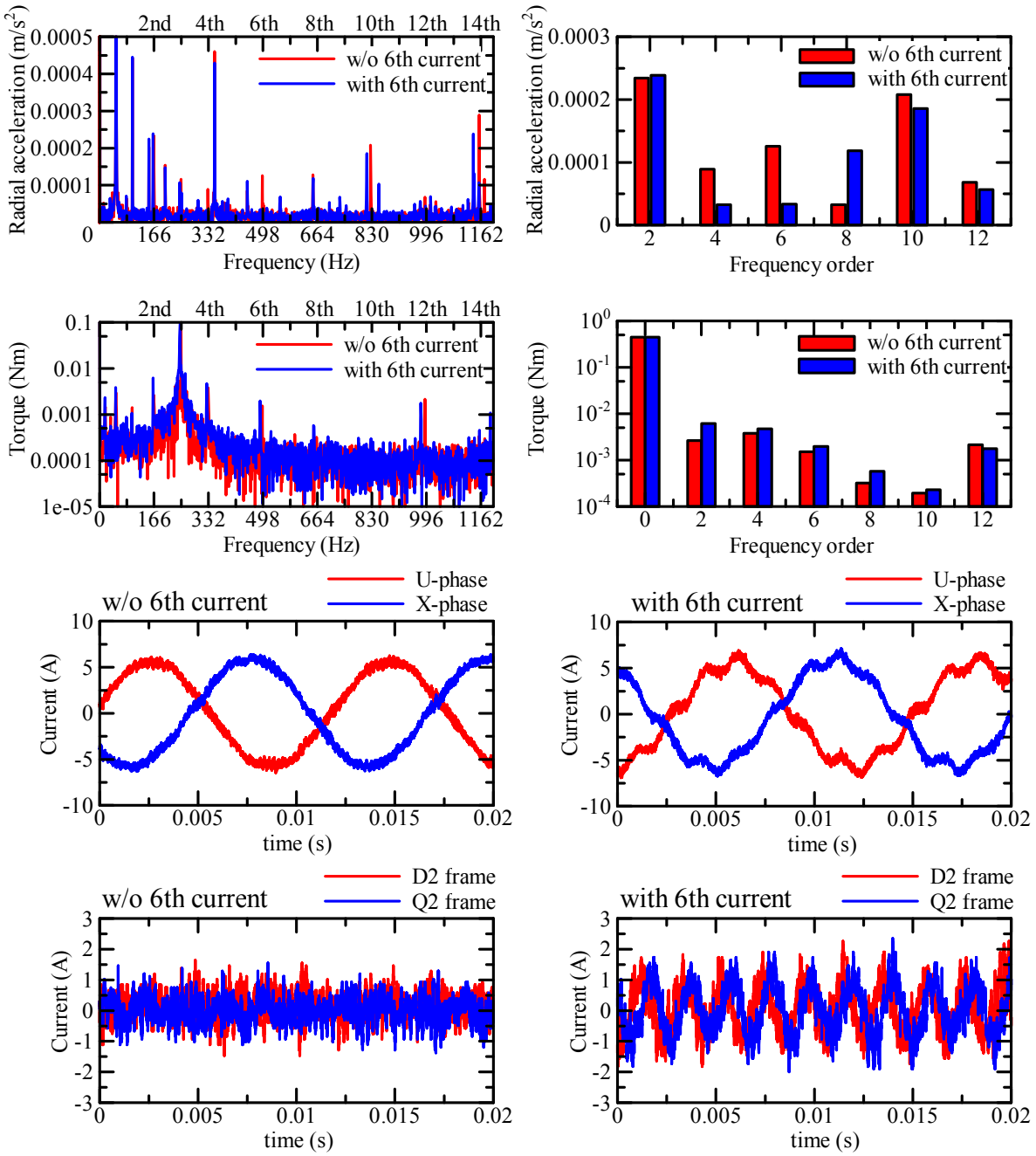

Fig. 7. Experiment results of radial force harmonic contents (upper graphs), torque harmonic contents (middle graphs), steady-state U-phase and X-phase current (upper middle graphs), and steady-state current in D2-Q2 reference frames (lowwer middle graphs).

TABLE II
MACHINE PARAMETERS AND EXPERIMENT CONDITIONS

Symbol	Quantity	Parameter
N	Machine speed	1000 rpm
P_n	Pole pairs	5
S	Slot number	12
n	Winding turns	8
I_{D1}	I_{D1} reference	0 A
I_{Q1}	I_{Q1} reference	-10 A
I_{6th}	6th current amplitude	1.0 A
θ_{6th}	6th current phase	305 deg
α	Winding displacement	-150 deg
V_{dc}	DC voltage	12 V
f_s	Switching frequency	20 kHz
L_{D1}	D1 inductance	55.7 μH
L_{Q1}	Q1 inductance	86.7 μH
L_{D2}	D2 inductance	61.4 μH
L_{Q2}	Q2 inductance	46.1 μH

Fig. 7 presents the results of harmonic analysis of radial direction acceleration, harmonic analysis of torque, the steady-state waveform of the phase current, and the steady-state waveform of the current in D2-Q2 frames obtained

by the experiment. Since the current in D2-Q2 frames cannot be measured directly, it is output using the DAC function of the microcontroller used for machine control. The sixth-order component of the radial acceleration was improved from 1.26×10^{-4} m/s^2 to 3.36×10^{-5} m/s^2, and a reduction of 73.3 % was confirmed. On the other hand, the sixth-order torque ripple is 1.53×10^{-3} Nm (w/o 6th current) and 1.97×10^{-3} Nm (with 6th current), which is extremely small compared to the main torque component.

The peaks near 250 Hz in the torque harmonic analysis

*

waveform are considered to be caused by the mechanical resonance of the machine bench. The reason why the suppression current of the sixth-order radial force is significantly different between the simulation and the actual experiment is considered as follows: As a premise, the resultant force of the sixth-order radial force of the double-winding machine with winding displacement cancels out in the ideal state because the stresses generated from each winding sets are 180° out of phase. However, in an actual machine, the component transmitted to the surface of the case is not zero because the case is not rigid and the structure is asymmetric, and vibration due to stress propagates. Since these cancellations occur, it is considered that the amplitude of the harmonic current differs between the simulation evaluated by stress and the experimental result evaluated by case vibration.

VI. CONCLUSIONS

This paper has proposed a system that reduces the sixth-order radial force and sixth-order torque ripple for the purpose of reducing vibration and noise caused by PMSM. Sixth-order torque ripple is suppressed by the structure by using an independent double three-phase PMSM with an odd number of pole pairs with a winding deviation of 30 degrees mechanical angle. The sixth-order radial force is suppressed by superimposing the sixth-order harmonic current on the redundant degrees of freedom of the two currents that are increased by adopting the double three-phase PMSM.

In the simulation, the electromagnetic excitation force applied to the central tip of the U-phase tooth was representatively measured, and the harmonic analysis was used to evaluate the sixth-order radial force. It was confirmed that the sixth-order radial force was suppressed by superimposing the sixth-order radial force was suppressed by 98.9 % by superimposing the sixth-order harmonic current. On the other hand, it was confirmed that the sixth-order torque ripple was smaller than the zeroth-order component, which is the main torque component, and the twelfth-order component, and it was confirmed that it was suppressed by the machine structure.

In the experiment, it was impossible to directly measure the radial force applied to the tooth, therefore the radial acceleration on the machine case surface was evaluated. It was confirmed that the sixth-order radial acceleration was reduced by 73.3 % by superimposing the sixth-order current. The sixth-order torque ripple is smaller than the main torque component and the twelfth-order component as in the simulation. Therefore, it is constrained by the structure.

REFERENCES

[1] R. Takahata, S. Wakui, K. Miyata, K. Noma, and M. Senoo, “Influence of Rotor Eccentricity on Vibration Characteristics of Permanent Magnet Synchronous Motor”, *IEEJ Journal of Industrial Applications,* Vol.8, No.3, pp.558-565 (2019)

[2] Y. Kawai, H. Haga, and S. Kondo: “Power Inverter Based Comparison of Torque Ripple Suppression in IPMSM with Concentrated Winding”, *IEEJ Transaction on Industry Application*, Vol.134, No.2 pp.127-138 (2014) (in Japanese)

[3] Z. Q. Zhu, Z. P. Xia, L. J. Wu and G. W. Jewell, "Analytical Modeling and Finite-Element Computation of Radial Vibration Force in Fractional-Slot Permanent-Magnet Brushless Machines", *IEEE Transactions on Industry Applications*, vol. 46, no. 5, pp. 1908-1918, Sept.-Oct. 2010

[4] Y. Asano, Y. Honda, Y. Takeda, and S. Morimoto: “Reduction of Vibration on Concentrated Winding Permanent Magnet Synchronous Motors with Considering Radial Stress”, *IEEJ Transaction on Industry Application*, Vol.121, No.11 pp.1185-1191 (2001) (in Japanese)

[5] H. Yashiro, and H. Takeda, “Reduction of a Radial Electromagnetic Oscillating Force of an Electrical Motor by Superposing a High Order Current”, *Transactions of the Japan Society of Mechanical Engineers Series C*, Vol.72, No.715, pp.723-728, (2006) (in Japanese)

[6] Kazuo Ohnishi, “Cogging Torque Reduction in Permanent Magnet Brushless Motors”, *IEEJ Transaction on Industry Application*, Vol.122, No.4 pp.338-345 (2002) (in Japanese)

[7] S. Shinnaka, and H. Kishida, “New Simple Torque-Sensorless Torque Control for Quasi-Perfect Compensation of 6th Harmonic Torque Ripple Due to Nonsinusoidal Distribution of Back EMF of PMSM”, *IEEJ Transaction on Industry Application*, Vol.131, No.8 pp.1068-1077 (2011) (in Japanese)

[8] M. Watahiki, T. Mori, L. Lan, J. Tanaka, T. Ueda, T. Fukumura, M. Kanematsu, and H. Fujimoto: “Reduction of Sixth-order Radial Force by Harmonic Current Control and its Application to EPS Motors”, *IEEJ Transaction on Industry Application*, Vol.139, No.8 pp.708-716 (2019) (in Japanese)

[9] Y. Oto, and T. Noguchi,” Fault-Tolerant Function of DC-Bus Power Source in A Dual Inverter Drive System and Its Operation Characteristics”, *IEEJ Journal of Industrial Applications,* Vol.8, No.6, pp.953-959 (2019)

[10] M. Shamsi-Nejad, B. Nahid-Mobarakeh, S. Pierfederici and F. Meibody-Tabar, "Fault Tolerant and Minimum Loss Control of Double-Star Synchronous Machines Under Open Phase Conditions", *IEEE Transactions on Industrial Electronics*, vol. 55, no. 5, pp. 1956-1965, May 2008

[11] T. Suzuki, Y. Hayashi, H. Kabune and N. Ito, "Pulsewidth Modulation Control Algorithm for a Six-Phase PMSM: Reducing the Current in the Inverter Capacitor and Current Sensing With Resistors", *IEEE Transactions on Industrial Electronics*, vol. 66, no. 6, pp. 4240-4249, June 2019

[12] T. Suzuki, H. Kabune, and N. Ito: “Minimum Peak Current Maximum Torque of Dual Winding Motor”, *IEEJ Transaction on Industry Application*, Vol.136, No.8 pp.532-539 (2016) (in Japanese)

[13] S. Kallio, M. Andriollo, A. Tortella and J. Karttunen, "Decoupled d-q Model of Double-Star Interior-Permanent-Magnet Synchronous Machines", *IEEE Transactions on Industrial Electronics*, vol. 60, no. 6, pp. 2486-2494, June 2013

[14] J. Karttunen, S. Kallio, P. Peltoniemi, P. Silventoinen and O. Pyrhönen, "Decoupled Vector Control Scheme for Dual Three-Phase Permanent Magnet Synchronous Machines", *IEEE Transactions on Industrial Electronics*, vol. 61, no. 5, pp. 2185-2196, May 2014

[15] C. Liu, F. Blaabjerg, W. Chen and D. Xu, "Stator Current Harmonic Control With Resonant Controller for Doubly Fed Induction Generator", *IEEE Transactions on Power Electronics*, vol. 27, no. 7, pp. 3207-3220, July 2012